PERGAMON

Vision Research 41 (2001) 2235–2243

Vision Research

www.elsevier.com/locate/visres

Stereoprocessing of cyclopean depth images: horizontally elongated summation fields

Christopher W. Tyler *, Leonid L. Kontsevich

Smith-Kettlewell Eye Research Institute, 2318 Fillmore Street, San Francisco, CA 94115, USA

Received 4 January 2000; received in revised form 14 June 2000

Abstract

The study evaluated how the detection efficiency varies with the length and width of Gabor wavelets of depth ripple in random element patterns. For local (one-cycle) wavelets, there was no anisotropy with respect to wavelet orientation, implying equal efficiency for processing shear versus compression disparities at threshold. The processing for larger patterns of depth ripple did not correspond to a fixed summation field but varied in size with spatial frequency, and in shape with orientation of depth ripples, up to four cycles of a horizontal bar at 0.5 cy/deg, or 8° of visual angle. The presence of such extended summation fields in only one orientation is incompatible with the idea of local attentional processing, with a single disparity channel or with an adaptive mechanism that could accommodate to any form of disparity image. Thus, these results suggest the presence of a multichannel hypercyclopean level of processing specialized for horizontal depth contours, whose only disparity information is in their surface texture.

Keywords: Stereopsis; Depth; Summation; Spatial; Gabor

1. Introduction

The purpose of the study was to determine the local processing structure for the depth form in complex visual scenes. In his random-dot stereograms, Julesz (1960) introduced the concept of a depth image that was not accompanied by any coherent monocular form information. The form of the depth image could be specified arbitrarily while the monocular dots in each remained entirely random. Actually, the idea had been developed much earlier by Santiago Ramon y Cajal at the end of the last century (Bergua & Skrandies, 2000) and by Kompaneysky (1939) in a hand-generated image of a face, but Julesz provided the means of accurate control to eliminate any monocular form information by mathematical randomization.

We approached this issue by evaluating the detection of sinusoidal ripples in the stereoscopic disparity of a noise field. Local processing of depth structure may be understood in terms of the effective receptive fields for processing the form information in a disparity field. The local disparity detectors provide the information as to the depth profile over space, together with a 'depth-cleaning' stage to resolve the ambiguities of multiple correspondence among the large number of dots in a random element stereogram. The result is (usually) a unitary depth surface. But having obtained the surface, the visual system is faced with the problem of 'understanding' or processing the form of this surface.

Since there is no monocular form information, Julesz (1971) posed the question of what mechanisms were available to gauge the form of the depth profile. This is actually a general question in human vision: once one goes beyond the low-level processing filters, how is the higher structure of forms, patterns and symmetries appreciated? The range of forms that we can categorize seems too large to propose elaborated filter mechanisms for each one, but it is hard to envisage the structure of an active system that could perform the same task. Recordings from monkey inferotemporal cortex tend to support the elaborated filter concept. Gross, Rocha-Miranda, and Bender (1972), Tanaka, Saito, Fukada, and Moriya (1991), Booth and Rolls (1998) and Hasselmo, Rolls, Baylis, and Nalwa (1989), report single cell (and local multiple unit) responses that are narrowly tuned

* Corresponding author. Fax: +1-415-3458455.
E-mail address: cwt@skivs.ski.org (C.W. Tyler).

0042-6989/01/$ - see front matter
PII: S0042-6989(00)00261-3

to highly specific types of stimuli, such as monkey eyes, faces and hands or a variety of common objects, with little response to spatially similar stimuli that are lacking some key property. Thus, it appears that cortical processing pursues the filter strategy up to several levels beyond the simple and complex cells of Hubel and Wiesel (1968).

To address the issue of how depth images are encoded, we performed a simple depth detection task for elongated targets of various kinds. This study was inspired by the Watson, Barlow, and Robson (1983) study of the optimal properties for detection of spatial contrast, but for the cyclopean depth detection task (i.e. 'what does the eye see best in depth?'). The first issue in such an enterprise is to establish the elongation structure for detection of depth in disparity forms. This goal is approached by obtaining a psychophysical estimate of the shape of the cyclopean summation mechanism operating for the detection of cyclopean shapes. (In this initial survey of the domain, we did not attempt to perform the full optimization to identify the best such 'receptive field' shape.) This summation shape may be formalized in terms of Gabor wavelet modulation of the horizontal binocular disparity information, $z(\phi, \theta)$ around a frontoparallel base plane in a filtered-noise image field. The Gabor disparity modulation is defined by:

$$z(\phi,\theta) = d\cdot e^{-(\phi/2\sigma_l)^2}\cdot e^{-(\theta/2\sigma_w)^2}\cdot\cos(f\theta) \quad (1)$$

with respect to orthogonal coordinates (ϕ, θ) in visual space, rotated to control the orientation θ of the cosine carrier modulation of the Gabor (where σ_l and σ_w are the standard deviations of the Gaussian envelope in the length and width with respect to the carrier orientation θ, f is the carrier ripple frequency and d is the horizontal disparity amplitude). Thus, instead of presenting a packet of spatiotemporal contrast modulation, we ask observers to discriminate a packet of spatiotemporal disparity modulation from a flat fixation plane. An example of a horizontal cyclopean Gabor wavelet is provided in the three-panel, filtered-noise stereogram of Fig. 1. It is intended to be viewed by free-fusion across the pairs of images. The Gabor should appear with the central peak in front or behind the background plane on the two sides, with the sign depending on whether the free-fusion was binocularly crossed or uncrossed.

The specific question addressed was how the detection efficiency varied with the length σ_l and width σ_w of the Gabor at different carrier orientations. Five hypotheses were envisaged as to how different underlying processing constraints would affect these summation properties in cyclopean space. Note that these hypotheses do not address the types of mechanism that exist in the brain in general, but the mechanism that determines the specific processing constraints measured by our data.

(1) A local *attentional* tracking system. One may conceive of an attentional focus tracking the derived depth surface, encoding its properties in the fashion that an aeroplane navigator might encode the topography of some countryside over which the aeroplane is flying. The encoding would form some sort of list of coordinates for features of interest, together with of conceptual encoding of the stimulus to be detected as, for example, 'a pair of long thin bars of vertical orientation' or 'a triangular hole in the base depth plane'. Such encoding should be very general and fail only when the image reaches some complexity limit. If the depth profile were appreciated by an active system of conceptual encoding in some form, there is no reason to suppose that it would have limitations specific to the local extent of the features. This attentional hypothesis therefore predicts no quantitative summing field limits.

(2) An *adaptive channel* system that can adjust itself for an ideal match to whatever disparity profile information is available in the depth image. Such a mechanism should exhibit ideal observer summation behavior for all configurations (subject to retinal inhomogeneity

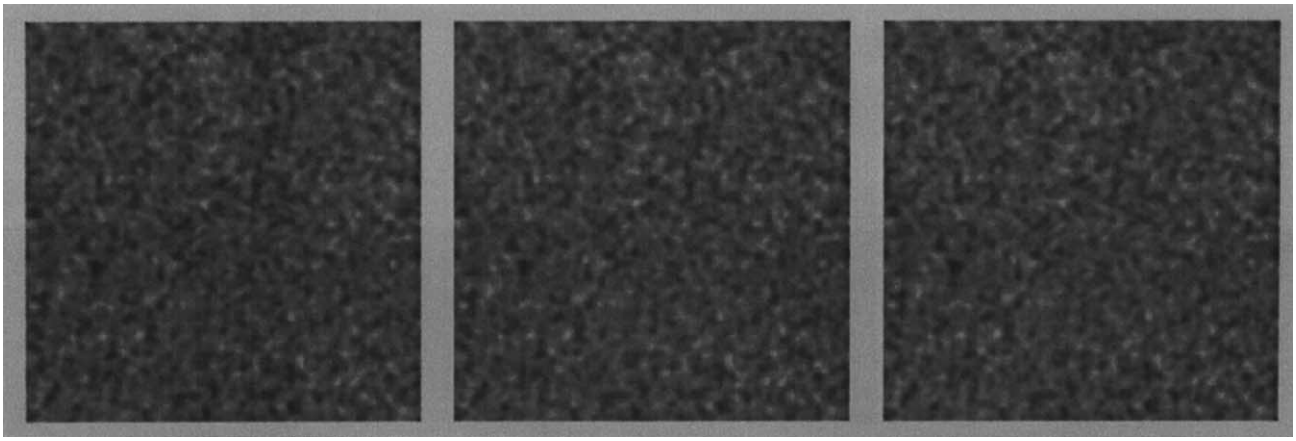

Fig. 1. Filtered noise stereogram of the cyclopean depth image of a horizontal Gabor wavelet.

constraints). That is, once threshold is established for the smallest cyclopean Gabor patch, detection should improve with the square root of area of the Gabor envelope, regardless of its shape.

The constraint of decreasing resolution outward from the foveal center would impose a decreasing efficiency with size, but one that would be uniform to orientation of the stereo information, either in the Gabor carrier or its envelope shape. However, the fact that the noise elements in typical stereoscopic stimuli are greatly above contrast threshold may mean that they overcome retinal variations in sensitivity. Previous work on stereosummation in terms of the upper depth limit (Tyler & Julesz, 1980) found that it conformed to ideal summation behavior up to several degrees.

(3) A *single-channel system* of generic summation fields across the cyclopean retina. Such summation fields would report in parallel some property such as local curvature of the depth image, from which the form of the depth image could be adduced. The summation fields would be analogous to a single layer of retinal receptive fields and should then have simple properties that are uniform with orientation. If the depth profile is processed by local filters operating on the cyclopean depth information, the filters may well be specialized for some forms of depth image rather than others.

If there is only one channel dominating detection at each location in the visual field, areal summation should have the particular form of asymptoting to linear improvement at small sizes and to size-independence at large sizes (Polat & Tyler, 1999; Chen & Tyler, 1999). We characterize this single-mechanism summation function as having $(-1, 0)$ asymptotes in double log coordinates. The intersection of the asymptotes would be independent of the carrier orientation or frequency in this generic channel hypothesis. Compare with hypotheses 2, 4 and 5.

(4) A *specialized channel system* where the form is processed by cyclopean receptive fields specific to particular aspects of the form of the depth image. Here the summation might differ in extent for different carrier orientations and the extent might vary in direction relative to each carrier orientation. However, for each combination of carrier orientation and summation direction, this hypothesis would invoke only one summation field at each field location. Thus, each summation function would have the same $(-1, 0)$ asymptotes as in Hypothesis 3, but with specialized variation of the asymptotes rather than a single fixed value.

(5) A *multiple channel system* of form processing where the form is processed by arrays of specific cyclopean receptive fields, similar to Hypotheses three or four, except that for each combination of carrier orientation and summation direction there would be multiple sizes of receptive field. Here the summation function would depart from the simple $(-1, 0)$ asymptote form. For example, if there was a range of summation fields of equal efficiency but different sizes, they should generate a range of summation behavior with a -0.5 slope on in double-log coordinates within that range, or $(-1, -0.5, 0)$ behavior (Tyler & Chen, 2000). (Such summation is found for luminance detection in the transition from Ricco's to Piper's laws, for example). This hypothesis differs from the adaptive channel hypothesis in that there could only be a limited set of channel arrays available, whereas an adaptive channel could in principle adapt to any form of stimulus (like learning specialized object configurations such as faces). Both Hypotheses predict the same summation slope for simple stimuli, however, so both are falsified if the data deviate from this slope.

In summary, measurement of the summation functions for various configurations of wavelet stimuli can reveal much about the underlying structure of the neural domain in which the wavelets are processed. In the present case, the wavelets are Gabors in the disparity domain, so they should help to reveal the local channel structure of form processing for depth images at a particular spatial frequency. In the course of this local processing evaluation, we also address the question of the sensitivity for depth ripple as a function of spatial frequency, first measured by Tyler (1973, 1974) and of relative sensitivity for different orientations of depth ripple, which was first measured by Rogers and Graham (1983). Although they found idiosyncratic differences among observers as a function of orientation, our main issue is the local structure at a particular frequency of depth ripple, which will be evaluated across the range of visible depth ripples for completeness.

2. Methods

2.1. Stimuli

Sinusoidal Gabor patches of cyclopean depth ripple (disparity wavelets) were generated in a filtered random-element stereoscopic display with a resolution of 1′ per pixel. To obtain subpixel resolution of disparity, the random base stimulus was filtered noise with a 7′ blur function and was set at a root mean square contrast of 50%. For all stimuli the Gabor ripple was defined by horizontal disparity variation of the base stimulus around the mean background level. The Gabors were all even-symmetric, and presented in either cosine or −cosine phase. An example of a Gabor disparity profile of the kind used for the study is shown in Fig. 1. The ripple could be horizontal or vertical and the envelope could have its major axis horizontal or vertical but the disparity was always horizontal (i.e. a

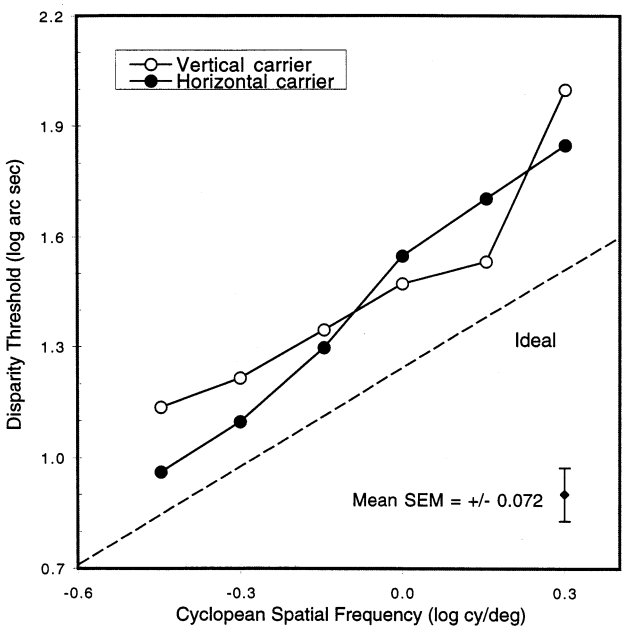

Fig. 2. Mean cyclopean modulation threshold function (MTF) for one-cycle Gabors with vertical (open symbols) and horizontal (filled symbols) depth ripples. Error bars depict ± one standard error of the means for the two observers. Note monotonic form of cyclopean spatial frequency tuning over the measured range and lack of a significant effect of carrier orientation for these local disparity stimuli. Axes in this and subsequent graphs scaled in octaves (0.3 $\log_{10}$ units).

primary binocular depth stimulus). The noise field in the experiments was 10.5° wide by 16° high, presented for 500 ms from a blank equiluminant field with a luminance of 35 cd/m^2. The independent variable was the amplitude of disparity required to achieve the detection criterion.

2.2. Procedure

The observer's task was to discriminate whether the central peak was forward or back from the mean disparity of the background. Disparity amplitude thresholds for front/back depth discrimination were determined by our maximum likelihood Ψ staircase (Kontsevich & Tyler, 1999) as a function of width and height of the cyclopean Gabor, for both horizontal and vertical carrier waveforms of the cyclopean bar carriers, over a full range of carrier spatial frequencies. The cyclopean Gabor targets had envelope widths of either one cycle (in terms of the envelope width at half-height) in both directions, one cycle vertically by eight cycles horizontally, or eight cycles vertically by one horizontally. The same paradigm was employed for cyclopean Gabor targets with horizontal ripples and for those with vertical ripples. Three thresholds were averaged for each stimulus condition.

To characterize the summation functions more fully, disparity thresholds were then measured as a function of envelope width or height for cyclopean Gabor targets with ripple frequencies of 0.5 and 2 cy/deg with both horizontal and vertical ripples. The envelope in the nonvarying dimension was one cycle in each case. Note that, in both experiments, the field width did not permit the full extent of the Gabor to be displayed at the lowest ripple spatial frequencies. Thus, had the visual system been able to take full advantage of the extended information available, the functions should have tended to converge at the lower ripple frequencies. In fact, however, the measured functions were approximately parallel across ripple frequency, implying that sufficient information was available to measure the limits of stereodetection performance.

3. Results and discussion

The mean cyclopean modulation threshold function (cyclopean MTF) for a one-cycle cyclopean Gabor ripple at each orientation of the carrier modulation is shown in Fig. 2. Axes in this and subsequent graphs scaled in octaves, or factors of two, of spatial frequency or sensitivity (intervals of 0.3 $\log_{10}$ units) Thus, each increment of 0.3 log units represents a doubling or halving of the respective quantities. The two functions are similar and the apparent shape differences do not reach statistical significance. (Statistical significance was assessed throughout the paper in terms of the t-test of comparisons between pairs of means. A difference between means was considered significant if it exceeded twice the standard deviation of the difference, computed from the sum of the variances of the two individual means. For $n = 3$, this criterion corresponds to a criterion level of $p < 0.05$).

The main feature of the frequency functions is that the thresholds continue to improve as cyclopean spatial frequency is reduced down to the lowest levels tested (0.35 cy/deg, or -0.45 log cy/deg.). In this respect, the wavelet data are similar to those for extended targets in showing maximum sensitivity at remarkably low spatial frequencies and a complete failure to detect the target above about 3 cy/deg, or 0.5 log cy/deg (Tyler, 1974; Rogers & Graham, 1983). However, there is a difference in that the peak spatial frequency for the extended cyclopean gratings was about 0.5 cy/deg, whereas the present work shows that for Gabor wavelets sensitivity peaks below 0.35 cy/deg. The difference is presumably attributable to the differences in available summation area, which is decreasing with the square of the spatial frequency in the present wavelet stimuli. The slope of the increase in spatial frequency corresponds to an ideal summation slope (dashed line, Fig. 2) of the square root of stimulus area (see Section 4). Note that the line is placed with an arbitrary vertical positioning, representing ideal summation behavior rather than ideal absolute efficiency.

Fig. 2 also provides a comparison between the sensitivities for horizontal and vertical depth ripples. For these two observers, there is no significant anisotropy at any ripple frequency for these one-cycle wavelets. This result leads to the important conclusion that there is no anisotropy between the processing of local shear versus compression gradients of horizontal disparity, since a horizontal ripple consists of shear disparities whereas a vertical ripple consists of compression disparities. As will be seen in the following figures, the anisotropy develops for wavelet targets larger than one cycle. In this sense, the remainder of the paper represents an exploration of the large-field anisotropy in terms of the cyclopean summation properties.

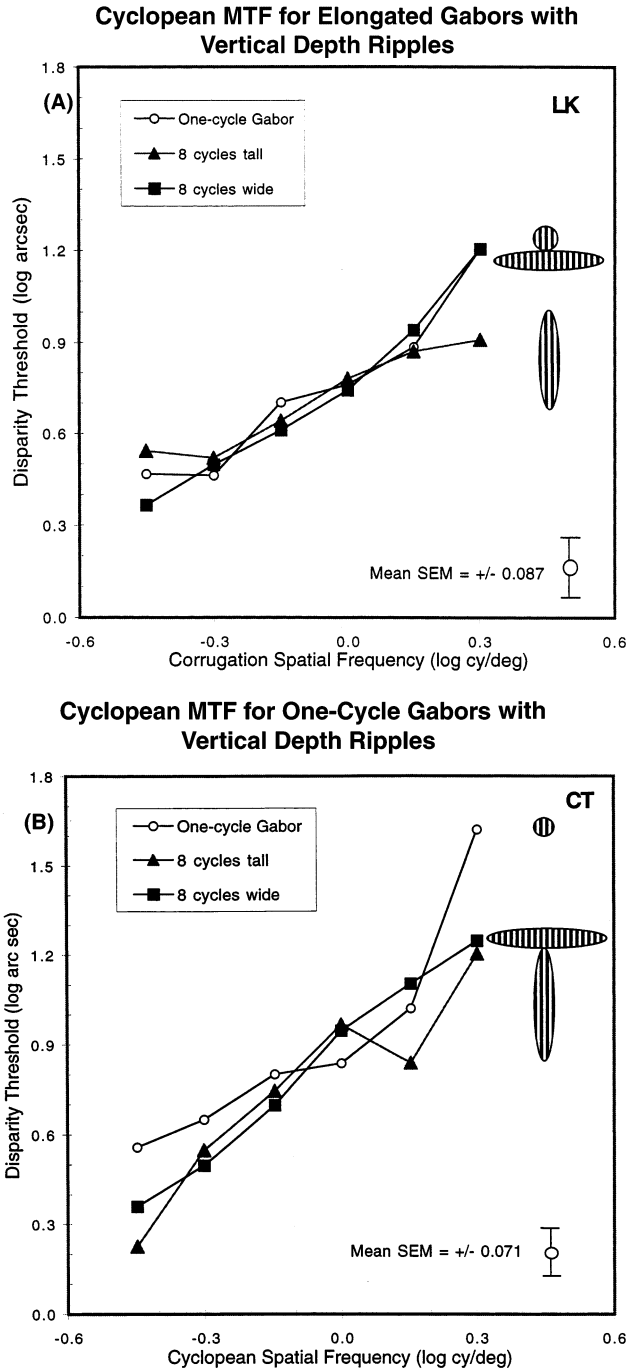

Fig. 3. Summation fields for vertical ripples. Left panel: observer LK; right panel: observer CT. The mean error of measurement is shown in each panel. The functions all coincide within the error of measurement, implying that there is no significant summation beyond the sensitivity for one cycle (open circles) in either direction.

The thresholds as a function of spatial frequency of the vertical ripples are shown for three elongation ratios separately for the two observers in Fig. 3. The functions are indistinguishable for the three configurations within the range of the measurement noise (about ± 0.1 log units of disparity). This result implies that the summation units for vertical ripples are limited to about one cycle in both directions, since providing an additional eight cycles of width or height generates no significant improvement in the detectability of the patch.

For summation over horizontal ripples, the picture is more interesting (Fig. 4). For observer LK, statistically significant summation in the vertical direction (across ripples) is substantial, averaging 0.2 log units with no significant variation across ripple frequency. In the horizontal direction (along ripples) even greater summation occurs, about 0.4 log units at all ripple frequencies. Thus, the summation is anisotropic to the horizontal ripple orientation. Observer CT shows similar behavior for horizontal elongation but very little summation in the vertical direction.

To interpret the summation revealed in Fig. 4, we would need to know whether summation proceeds according to the single channel model (log slope of -1) or the ideal observer model of multiple receptive fields up to the summation size, which proceeds with a log slope of -0.5 (Kersten, 1984; Tyler & Chen, 2000). Size summation data were therefore obtained for observer LK at the depth ripple frequencies of 0.5 and 2 cy/deg for all four pattern configurations (Figs. 5 and 6).

The aspect ratio data of Fig. 5 confirm the result of Fig. 3 that there is very little summation beyond one cycle for vertical depth ripples. The paradigm of Fig. 5 is replicated in Fig. 6 for horizontal depth ripples. At 2 cy/deg the summation along the ripples is maximal at an aspect ratio of 4:1 cycles (0.6 log units). In terms of the individual bars of the depth ripple, this result corresponds to an aspect ratio of 8:1 for the length of the half-cycle bars in the stimulus. Interestingly, very little summation was seen at the low spatial frequency (lower curves) until the divergence of the curves for the greatest elongation. The implication of this divergence is that the summation field at this low cyclopean frequency is about 10 cycles long, but the present display did not allow a full evaluation of its characteristics. Note that the quantitative value of this longest summation extent means little because the tails of the image

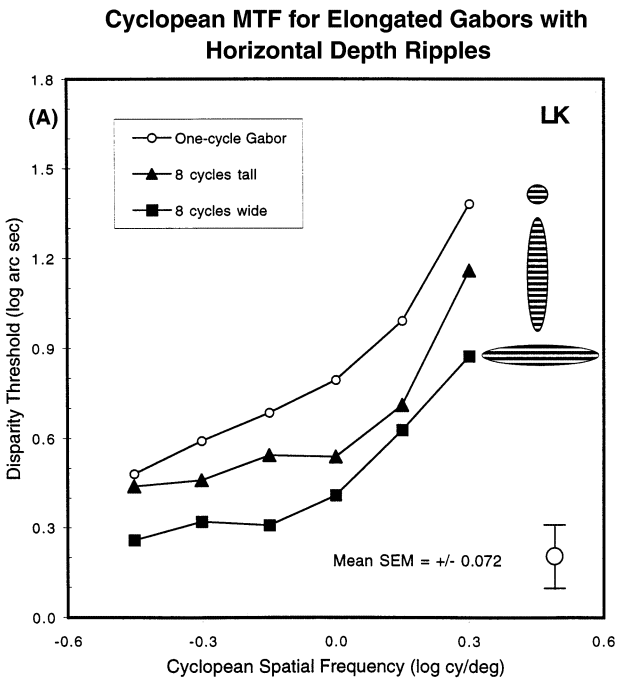

Fig. 4. Summation fields for horizontal depth ripples (otherwise as Fig. 3). There is significant summation in the horizontal direction at all cyclopean spatial frequencies (downward shift of filled squares) and also summation in the vertical direction for observer LK (smaller downward shift of filled triangles).

were cut off by the horizontal limits of the display at this low spatial frequency. It was considered worth going to this degree of elongation because the central 10° of the stimulus that could be depicted would reach increasing uniformity of disparity modulation, but the emergence of summation at and beyond this width was unanticipated.

4. Interpretation

The most extended summation fields for stereoscopic form may be depicted geometrically in a mesh plot (Fig. 7). For horizontal cyclopean ripples (H), horizontal summation extended to about eight (half-cycle) bar widths but vertical summation differed somewhat for

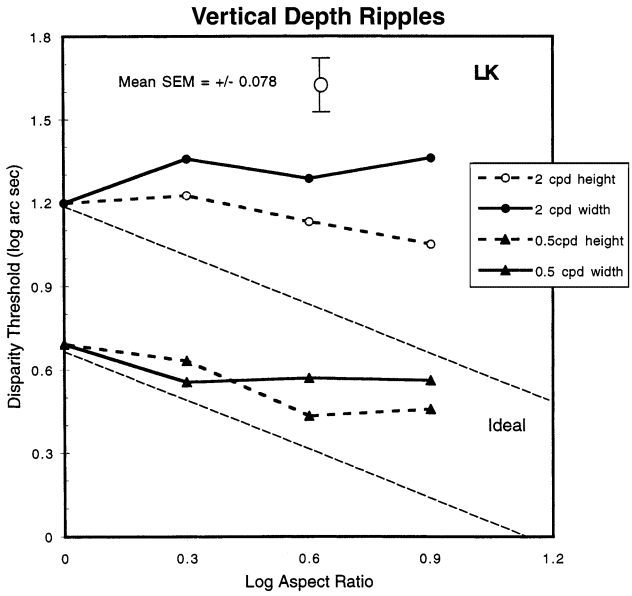

Fig. 5. Summation for vertical depth ripples as a function of aspect ratio for observer LK. Upper curves: 2 cy/deg. Lower curves: 0.5 cy/deg. Solid curves: summation over the height (vertical) direction, with the ripples. Dashed curves: summation over the width (horizontal) direction, orthogonal to the ripples. Slight collinear summation is seen at 0.5 cy/deg in the height direction. Thin dashed lines: slopes of -0.5 corresponding to Ideal Observer summation behavior.

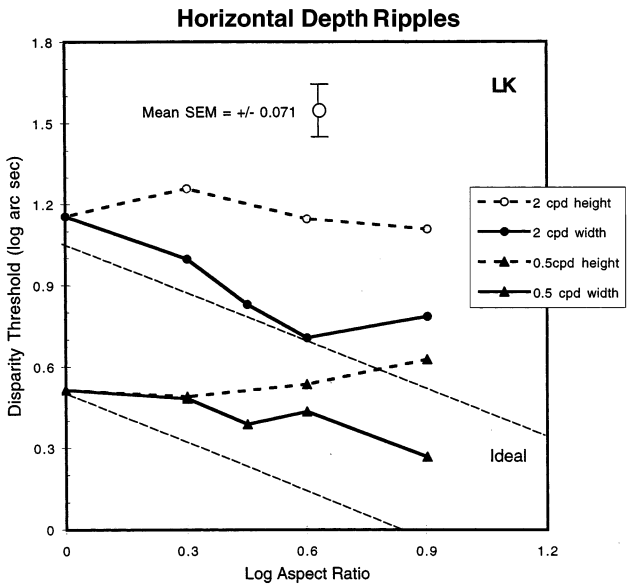

Fig. 6. Summation for horizontal depth ripples as a function of aspect ratio. Other details as in Fig. 5. Significant summation is seen only for the collinear direction at 2 cy/deg, up to an aspect ratio of 4:1.

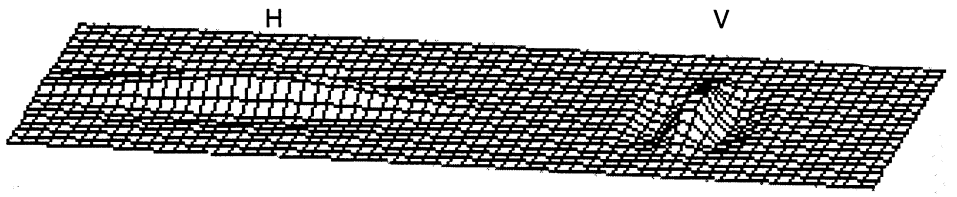

Fig. 7. Depiction of the inferred cyclopean field structure for horizontal (H) and vertical (V) disparity ripples (defined by horizontal disparity modulation).

the two observers, being minimal for one but extending up to two cycles for the other. The narrower of the two observers' functions is depicted. For vertical cyclopean ripples (V), both length and width summation were minimal beyond one cycle.

The data show that summation for depth information is not performed by:

- a local *attentional* tracking system, since the measured summing fields were of limited extent with idiosyncratic features. The only plausible constraint on an attentional tracking system is that it would show preferential tracking along stereoscopic ridges, but such a system would be isotropic to orientation, unlike the data of Fig. 4 vs. Fig. 3. It is also hard to envisage how attentional tracking would explain the different summation properties in each direction.
- an *adaptive channel* system, since the data were anisotropic. An adaptive channel that could adjust itself to whatever disparity profile information is available should show isotropic summation behavior with respect to both carrier and envelope information in the cyclopean Gabor stimuli. It should also show ideal summation behavior up to its limit.
- a system of *generic* summation fields (like those in the retina), since they again should be isotropic to both carrier and envelope information.
- a *multiple channel system* of form processing because the summation behavior observed does not conform to the Ideal Observer prediction of a $(-1, -0.5, 0)$ sequence of summation slopes. Such summation as is significant and has defined slopes makes a better match to the $(-1, 0)$, being steeper than the Ideal Observer slope of -0.5 at short widths and shallower at long widths (Fig. 6, upper solid curve).

We conclude that cyclopean depth ripples appear to be processed by a *specialized* channel system of form processing where the form is processed by cyclopean summation fields specific to particular aspects of the cyclopean form. The summation differs in extent both for different carrier orientations and for its direction over each carrier orientation. It is possible to concoct other correspondingly specialized explanations (such as an attentional mechanism that can only track horizontal ripples), but any such explanation would effectively be equivalent to the specialized channel hypothesis (e.g. a specialized 'attentional' channel).

Is it possible that the specialized summation structure reported here derives from the horizontal anisotropy of stereopsis, that fact that the eyes deliver depth signals predominantly in the form of horizontal rather than vertical disparities? This interpretation seems implausible to us for two reasons. The anisotropy implies a disparity gradient limit for horizontal changes in disparity (what we are calling vertical ripples) but no constraint whatever on vertical changes in disparity (horizontal ripples). The properties of disparity gradient limits might be stretched to imply a concurrent elevation in thresholds. Thus, the place that further summation might be needed would be in the vertical summation of vertical ripples, where it could compensate for the disruption of stereo processing by the horizontal gradients. However, very little summation seen for this vertical/vertical case.

The second reason for doubting the influence of the disparity anisotropy is that it would imply that the summation was required to bring thresholds into the same range for the impaired orientation as they were for the unimpaired orientation without summation. Thus, thresholds for horizontal depth ripples should be higher than for vertical with the smallest stimuli to justify the need for summation to bring them within the same range. In fact, however, thresholds were at least as low for the horizontal ripples even for the smallest cyclopean Gabors (Fig. 2). By the time the horizontal summation has occurred, thresholds were up to 0.5 log units better for horizontal than vertical ripples.

Thus, rather than deriving from a local anisotropy, the horizontal summation seems to be serving some purpose of specialized disparity processing. The fact that there is little vertical summation implies that the summation is not specialized for ripples per se, just for disparity ripples of all spatial frequencies in the horizontal direction. One possibility is that the specialization is to help overcome the deficiency of disparity processing for horizontal luminance contours. Objects such as vertical branches have well-defined, high-contrast vertical contours to support stereopsis. Horizontally contoured objects have only their surface texture to support stereoscopic depth localization because horizontal contours have no horizontal disparity. Thus there is a special need for horizontally elongated summation fields to summate the horizontal texture infor-

mation. The long horizontal fields found in our study, particularly sensitive to horizontal depth contours, would be ideal to help disambiguate the depth of horizontal branches. Early primates who lacked them might very well have literally dropped out of the gene pool.

Another possibility is that the horizontal summation is a specialization is for the horizon itself, where detailed depth information may be particularly useful (as when looking ahead while driving on the open road, for example). This hypothesis would suggest that the specialization could be local to the region extending on either side of the fovea, as opposed to a generic specialization for horizontal depth ripples throughout the macular region. It should also be particular for the depth form of the horizon, with a horizontal plane below meeting a vertical one above. Conversely, the horizontal contour hypothesis suggests that the elongated summation should occur equally at locations throughout the stereoscopic processing field, since horizontal contours are equally likely at all locations. These hypotheses suggest future directions for this line of research, to evaluate whether the elongated stereo summation matches the properties expected for a horizon or horizontal contour specialization.

4.1. What cyclopean target does the eye see best?

As mentioned in the introduction, one can use the relationship to the Ideal summation slope to determine what cyclopean target the eye sees best, in the sense of the visual efficiency measure defined by Watson, Watson, Barlow, and Robson (1983). In terms of the spatial-frequency variable, the fixed-cycle design means that the area of the stimuli is varying with the square of the spatial frequency. Since ideal performance increases with area$^{-0.5}$, the line of constant efficiency corresponds to a slope of one (dashed line in Fig. 2). This means that small cyclopean targets are detected at roughly constant efficiency throughout the range of cyclopean spatial frequencies (although no attempt is made to calculate the absolute efficiency, i.e. the vertical placement of the efficiency line). Quantitatively, the highest efficiencies were measured for the horizontal ripples in the high frequency range, at 1.4 cy/deg for LK and at 2 cy/deg for CT (although this latter frequency is at the end of the measured range, so higher frequencies would need to be tested to determine whether this was the optimum frequency). For LK, the efficiency at 2 cy/deg for horizontal ripples increased up to a length equivalent to four cycles. For vertical ripples, threshold remained constant with elongation, meaning that efficiency was highest for the smallest stimuli.

The aspect-ratio data thus provide a general idea that the optimum is likely to be found at high frequencies of horizontal ripples about four cycles long, but the study was not structured with the goal of determining the optimum. The errors of measurement are too great to define statistically the optimum stimulation conditions (cf. Watson et al., 1983; Polat & Tyler, 1999). Considerable extra hunting is required to locate the minimum point in n-dimensional feature space, including varying the tinting for maximum efficiency. The present data could act as a starting point for such a study, but do no more than to suggest a good place to look for the best cyclopean target in their present form.

5. Conclusion

There is specialized processing for local patterns of cyclopean disparity. The structure of this processing does not correspond to a fixed summation field but varies in size with spatial frequency and in shape with orientation of the disparity ripples. The data imply the existence of length summation up to four cycles of a horizontal bar at 0.5 cy/deg, or 8° of visual angle. The presence of such extended summation fields controverts the notion of local attentional processing. The radical change in summation properties with ripple orientation is incompatible with either the idea of local attentional processing or the idea of single-channel processing of some property of the disparity field. Finally, the limited summation for vertical ripples and anisotropic summation for horizontal ripples is inconsistent with the concept of an adaptive mechanism that can accommodate to any tractable form of disparity image.

Thus, these results imply the existence of a channel-based hypercyclopean level of processing for aspects of cyclopean form. The only hypothesis that seems to account for the diverse summation properties, and the self-scaling of the MTF with ripple frequency, is a set of Gabor-type filters for the cyclopean form in the depth image, much like the classical receptive fields processing the luminance image in the retinotopic cortical areas. The specificity of the channel structure seems incompatible with a large supply of channels at each ripple frequency and orientation, and more consistent with specialized processing for common depth features such as horizontal branches or the earth's horizon.

Acknowledgements

My thanks to Scott Stevenson for his astute reading of an earlier draft. Supported by NIH grant EY 7890.

References

Bergua A., & Skrandies W. (2000). An early antecedent to modern random dot stereograms: 'The Secret Stereoscopic Writing' of Ramón y Cajal, *International Journal of Psychophysiology* (in press).

Booth, M. C., & Rolls, E. T. (1998). View-invariant representations of familiar objects by neurons in the inferior temporal visual cortex. *Cerebral Cortex*, *8*, 510–523.

Chen, C. C., & Tyler, C. W. (1999). Spatial pattern summation is phase insensitive in foveal but not in peripheral vision. *Spatial Vision*, *12*, 267–285.

Gross, C. G., Rocha-Miranda, C. E., & Bender, D. B. (1972). Visual properties of neurons in inferotemporal cortex of the Macaque. *Journal of Neurophysiology*, *35*, 96–111.

Hasselmo, M. E., Rolls, E. T., Baylis, G. C., & Nalwa, V. (1989). Object-centered encoding by face-selective neurons in the cortex in the superior temporal sulcus of the monkey. *Experimental Brain Research*, *75*, 417–429.

Hubel, D. H., & Wiesel, T. N. (1968). Receptive fields and functional architecture of monkey striate cortex. *Journal of Physiology (London)*, *195*, 215–243.

Julesz, B. (1960). Binocular depth perception of computer generated patterns. *Bell System Technical Journal*, *39*, 1125–1162.

Julesz, B. (1971). *Foundations of Cyclopean Perception*. Chicago: University of Chicago Press.

Kompaneysky, B. N. (1939). Depth sensations: analysis of the theory of stimulation by non-exactly corresponding points. *Bulletin of Ophthalmology (USSR)*, *14*, 90–105 in Russian.

Polat, U., & Tyler, C. W. (1999). What pattern the eye sees best. *Vision Research*, *39*, 887–895.

Rogers, B. J., & Graham, M. E. (1983). Anisotropies in the perception of three-dimensional surfaces. *Science*, *221*, 1409–1411.

Tanaka, K., Saito, H., Fukada, Y., & Moriya, M. (1991). Coding visual images of objects in the inferotemporal cortex of the macaque monkey. *Journal of Neurophysiology*, *66*, 170–189.

Tyler, C. W. (1973). Stereoscopic vision: cortical limitations and a disparity scaling effect. *Science*, *181*, 276–278.

Tyler, C. W. (1974). Depth perception in disparity gratings. *Nature*, *251*, 140–142.

Tyler, C. W., & Chen, C.-C. (2000). Signal detection theory in the 2AFC paradigm: Attention, channel uncertainty and probability summation. *Vision Research*, *40*(23), 3245–3255.

Tyler, C. W., & Julesz, B. (1980). On the depth of the cyclopean retina. *Experimental Brain Research*, *40*, 196–202.

Watson, A. B., Barlow, H. B., & Robson, J. G. (1983). What does the eye see best? *Nature*, *302*, 419–422.